JOURNAL OF COMPUTATIONAL PHYSICS 116, 154–159 (1995)

Atom-Centered Functions in the Optimized Thomas–Fermi Theory

GARY G. HOFFMAN

Department of Chemistry, Florida International University, Miami, Florida 33199

Received September 4, 1993; revised May 10, 1994

In the application of the optimized Thomas–Fermi theory to condensed phase systems, it has proved convenient to introduce a sum of atom-centered functions to represent the most rapidly varying part of the electron density near the nuclei. By extraction of this portion of the density, attention can be focused on the more slowly varying portion, allowing numerical techniques to be employed without being hindered by a prohibitively high density of grid points. Dealing with these atom-centered functions is facilitated by the closed-form evaluation of some nontrivial integrals. For the case of exponential functions, these integrals are evaluated here and specific methods for their computation are presented. © 1995 Academic Press, Inc.

1. INTRODUCTION

With the goal of generating electron densities for condensed phase systems, the *optimized Thomas–Fermi* (OTF) theory [1, 2] was derived. The theory is based on a path integral description of the many-electron system and expresses the electron density in a way that does not rely on the construction of a many-electron wave function. The beauty of the theory is that the computation of an electron density increases in effort only linearly with the size of the system, and not with a higher order dependence as in wave function based theories. Even if the OTF theory is ill-suited to smaller systems (as it is), it becomes preferable as the system gets larger. The application to condensed phase systems is therefore a natural one.

Preliminary calculations have indicated that the OTF theory provides accurate electron distributions in some simple many-electron systems [1, 3]. Efforts are now under way to develop methods for studying condensed phase systems with this theory. In the process, a number of computational details must be worked out. One such detail is worked out in this paper.

The OTF equations can be written

$$\rho(\mathbf{r}) = \frac{\kappa^3(\mathbf{r})}{3\pi^2}\,\eta(\kappa^2(\mathbf{r})) \tag{1a}$$

$$\kappa^2(\mathbf{r}) = \frac{2m}{\hbar^2}\left\{\varepsilon_F - \frac{\kappa(\mathbf{r})}{2\pi}\int \frac{j_1(2\kappa(\mathbf{r})|\mathbf{r}-\mathbf{r}'|)}{|\mathbf{r}-\mathbf{r}'|^2}\,v(\mathbf{r}')\,d^3r'\right\}, \tag{1b}$$

where ε_F is the Fermi energy of the system, $v(\mathbf{r})$ is the effective one-electron potential, $\eta(z)$ is the Heaviside function, and $j_1(z)$ is the spherical Bessel function of the first kind of order 1. Formula (1a) is identical in form to the Thomas–Fermi equation [4, 5]. The difference here is in the specification of the function, $\kappa(\mathbf{r})$. In Thomas–Fermi theory, the density depends on the potential, $v(\mathbf{r})$, only at the position under consideration. In OTF theory, the density depends on the potential in a region about the position under consideration [1]. As a result, OTF theory does not have the shortcomings of the Thomas–Fermi theory.

The OTF theory is generally applied within the framework of density functional theory [6]. In this framework, the effective potential is expressed as

$$v(\mathbf{r}) = v_{\text{ext}}(\mathbf{r}) + \phi(\mathbf{r}) + v_{\text{xc}}[\rho, \mathbf{r}], \tag{2}$$

where the first term on the right-hand side is the externally applied potential (such as an applied magnetic or electric field), the second is the Coulomb potential due to both the nuclei and the averaged electron distribution, and the final term is referred to as the "exchange-correlation potential." In essence, density functional theory proves that there exists a unique exchange-correlation potential, $v_{\text{xc}}[\rho, \mathbf{r}]$, that depends on the electron density (not the wave function explicitly), such that solution of the independent-electron problem with the potential above gives the correct electron density for the system. Although the formal definition of the exchange-correlation potential cannot be applied in practice, a number of useful approximations exist [7].

One method for applying these formulas to condensed phase systems involves numerical solution of the equations. We have made some effort to develop a code to perform calculations of this type and have found it convenient to separate the electron density into two parts, a sum of atom-centered functions plus a density deformation:

$$\rho(\mathbf{r}) = \sum_J \rho_J^0(\mathbf{r} - \mathbf{R}_J) + \delta\rho(\mathbf{r}). \tag{3}$$

The sum is over all the atoms in the system, appropriately cut off for condensed phase systems. The functions $\rho_J^0(\mathbf{r})$ are known, preferably analytic in form, and are designed to model

0021-9991/95 $6.00

the core portions of the atomic densities. The quantities $\mathbf{R}_J$ are the nuclear positions of the atoms. The advantage of this separation is that the atom-centered functions are expected to contain the major variations in the density about the nuclei. This means that the function $\delta\rho(\mathbf{r})$ is relatively smooth, making it easier to handle by numerical means.

An alternate method of applying these formulas is to expand the density in a bilinear form of atom-centered basis functions, the coefficients being optimized to give the best agreement with the OTF equations. This would correspond to a linear combination of atomic orbitals (LCAO) approach to solving the OTF equations. Both this and the numerical methods are now under investigation.

With the introduction of the atom-centered functions, a separation can also be applied to Eq. (1b), one part being associated with the atom-centered portion of the density and the other with what is left. Specifically, define $\phi_J^0(\mathbf{r})$ as the Coulomb potential associated with nucleus J (assumed to be at the origin) and the atom-centered electron density, $\rho_J^0(\mathbf{r})$. It is the solution of the Poisson equation

$$\nabla^2\phi_J^0(\mathbf{r}) = 4\pi\{Z_J\delta(\mathbf{r}) - \rho_J^0(\mathbf{r})\}, \tag{4}$$

subject to the appropriate boundary conditions. Equation (1a) can now be written as

$$\kappa^2(\mathbf{r}) = \frac{2m}{\hbar^2}\left\{\varepsilon_F + \sum_J I_J^0(\kappa(\mathbf{r}), \mathbf{r} - \mathbf{R}_J) - \frac{\kappa(\mathbf{r})}{2\pi}\int\frac{j_1(2\kappa(\mathbf{r})|\mathbf{r}-\mathbf{r}'|)}{|\mathbf{r}-\mathbf{r}'|^2}\{\delta\phi(\mathbf{r}') + v_{xc}(\mathbf{r}')\}\,d^3r'\right\}, \tag{5}$$

where

$$I_J^0(\kappa, \mathbf{r}) = -\frac{\kappa}{2\pi}\int\frac{j_1(2\kappa|\mathbf{r}-\mathbf{r}'|)}{|\mathbf{r}-\mathbf{r}'|^2}\phi_J^0(\mathbf{r}')\,d^3r'. \tag{6}$$

It is desirable to have the atom-centered densities accurately model the electron distributions near the nuclei, where the overall density varies most rapidly. When this is true, the major variations of the right-hand side of Eq. (5) are contained in the functions $I_J^0(\kappa, \mathbf{r})$, and the remaining integral should be relatively easy to handle by numerical means. As is often the case in computational work, the evaluation of an integral is most easily done if some closed-form expression can be obtained for at least part of it. This is the goal for the functions in Eq. (6) using the specific atom-centered densities to be described next.

A convenient choice for the atom-centered densities is a sum of exponentials. Focusing on a single atom and dropping the index J for clarity, a typical atom-centered density can be written as

$$\rho^0(r) = \sum_\mu c_\mu e^{-\alpha_\mu r}, \tag{7}$$

the constants c_μ and α_μ being chosen based on some suitable criteria. If we require that the atom-centered density exactly screen the nuclear charge, the Coulomb potential associated with it is given by

$$\begin{aligned}\phi^0(r) &= \frac{e^2}{4\pi\varepsilon_0}\left\{-\frac{Z}{r} + \int\frac{\rho^0(r')}{|\mathbf{r}-\mathbf{r}'|}d^3r'\right\} \\ &= -\frac{e^2}{4\pi\varepsilon_0}\frac{4\pi}{r}\sum_\mu c_\mu\frac{(2+\alpha_\mu r)}{\alpha_\mu^3}e^{-\alpha_\mu r}.\end{aligned} \tag{8}$$

The contribution to the function defined in Eq. (5) is then

$$I^0(\kappa, r) = \frac{e^2}{4\pi\varepsilon_0}\sum_\mu\frac{4\pi c_\mu}{\alpha_\mu^3}G(\kappa, \alpha_\mu, r), \tag{9}$$

where

$$G(\kappa, \alpha, r) = 2J_1(\kappa, \alpha, r) + \alpha J_2(\kappa, \alpha, r) \tag{10a}$$

and

$$\begin{aligned}J_1(\kappa, \alpha, r) &= \frac{\kappa}{2\pi}\int\frac{j_1(2\kappa|\mathbf{r}-\mathbf{r}'|)}{|\mathbf{r}-\mathbf{r}'|^2 r'}e^{-\alpha r'}\,d^3r' \\ J_2(\kappa, \alpha, r) &= \frac{\kappa}{2\pi}\int\frac{j_1(2\kappa|\mathbf{r}-\mathbf{r}'|)}{|\mathbf{r}-\mathbf{r}'|^2}e^{-\alpha r'}\,d^3r'.\end{aligned} \tag{10b}$$

These non-trivial integrals are evaluated in this paper.

2. EVALUATION OF $J_1(\kappa, \alpha, r)$

As expressed above in the first one of Eqs. (10b), it is possible to evaluate the integral directly, first evaluating the angular integrals and then tackling the radial one. However, the integrand that results has an awkward form that depends on whether r or r' is greater and the indefinite integrals that result are complicated. The evaluation is made easier after a change in origin, followed by the introduction of an integral representation for part of the integrand.

Changing the origin of integration to $\mathbf{r}$,

$$J_1(\kappa, \alpha, r) = \frac{\kappa}{2\pi}\int\frac{j_1(2\kappa r')}{r'^2}\frac{e^{-\alpha|\mathbf{r}+\mathbf{r}'|}}{|\mathbf{r}+\mathbf{r}'|}d^3r'. \tag{11}$$

Assuming that $\alpha > 0$, as is true here, the following integral identity is valid:

$$\frac{e^{-\alpha|\mathbf{r}+\mathbf{r}'|}}{|\mathbf{r}+\mathbf{r}'|} = \frac{1}{2\pi^2}\int\frac{e^{i\mathbf{q}\cdot(\mathbf{r}+\mathbf{r}')}}{q^2+\alpha^2}d^3q. \tag{12}$$

With this identity introduced, the integrations over $\mathbf{r}'$ can be performed, so that Eq. (11) now becomes

$$J_1(\kappa, \alpha, r) = \frac{1}{4\pi} \int \frac{e^{i\mathbf{q}\cdot\mathbf{r}}}{q^2 + \alpha^2} g(q/2\kappa)\, d^3q, \tag{13}$$

where

$$g(z) = 1 + \frac{1}{2}\left(\frac{1}{z} - z\right) \ln\left|\frac{1+z}{1-z}\right|. \tag{14}$$

The function $g(z)$ is encountered in the application of the random phase approximation (RPA) to the degenerate electron gas [8]. It has singularities at $z = \pm 1$, where its derivative becomes infinite, but otherwise it is a well-behaved function. To properly deal with this function, it is useful to express it as the limit of an analytic function,

$$g(z) = \lim_{\eta \to 0} g_\eta(z), \tag{15}$$

where

$$g_\eta(z) = 1 + \frac{1}{4}\left(\frac{1}{z} - z\right) \ln\left[\frac{(1+z)^2 + \eta^2}{(1-z)^2 + \eta^2}\right]. \tag{16}$$

The function $g_\eta(z)$ has branch point singularities at the four points $z_{++} = 1 + i\eta$, $z_{+-} = 1 - i\eta$, $z_{-+} = -1 + i\eta$, and $z_{--} = -1 - i\eta$. In order to ensure that the function is analytic along the real axis (along which it is integrated), the branch cuts are chosen to extend from these points to infinity, in directions directly away from the real axis (see Fig. 1).

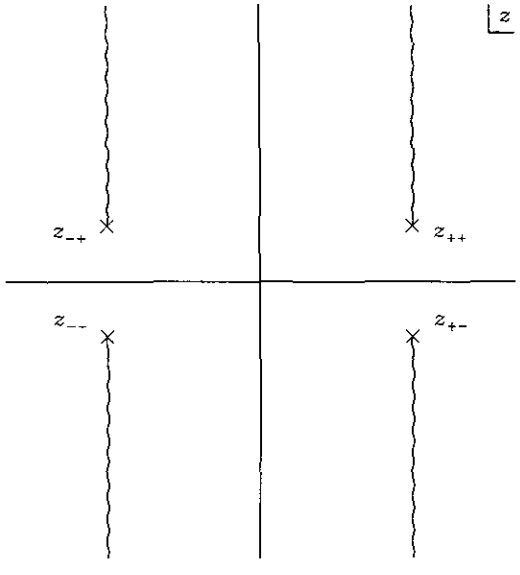

FIG. 1. Branch structure for the function $g_\eta(z)$, defined in Eq. (16) of the text.

The logarithm in the function $g_\eta(z)$ can be reexpressed as

$$\ln\left[\frac{(1+z)^2 + \eta^2}{(1-z)^2 + \eta^2}\right] = \ln\left[\frac{(z - z_{-+})(z - z_{--})}{(z - z_{++})(z - z_{+-})}\right]. \tag{17}$$

Defining r_{++} and θ_{++} as the magnitude and argument (or phase) of the complex number $(z - z_{++})$ and similarly for the other three terms, the logarithm can be expressed as

$$\ln\left[\frac{(1+z)^2+\eta^2}{(1-z)^2+\eta^2}\right] = \ln\left[\frac{r_{-+}r_{--}}{r_{++}r_{+-}}\right] + i(\theta_{-+} + \theta_{--} - \theta_{++} - \theta_{+-}). \tag{18}$$

The reason for going over this so carefully is that it is necessary to define the phases appropriately so that the function is strictly real along the real axis. This requires that the phase of θ_{++}, for instance, be zero when z is directly below z_{++}. That is, when $(z - z_{++}) = -ix$, with x real and positive, $\theta_{++} = 0$. Proceeding in this way, θ_{+-} is zero when z is directly above z_{+-} and similarly for the other two terms. It is readily shown that this choice of phase leads to a real function when z is real. In addition, this choice of phase leads to a useful expression when z is pure imaginary in the upper half z-plane. Specifically,

$$g(ix) = 1 + \left(\frac{1}{x} + x\right) \arctan(x), \quad x \geq 0. \tag{19}$$

This information allows Eq. (13) to be modified to a more convenient form. After performing the angular integrals and then noting that $g_\eta(z)$ is even in its argument, we find that

$$J_1(\kappa, \alpha, r) = \frac{1}{2ir} \lim_{\eta \to 0} \int_{-\infty}^{\infty} \frac{q g_\eta(q/2\kappa)}{q^2 + \alpha^2} e^{iqr}\, dq. \tag{20}$$

It is now possible to apply some of the techniques of contour integration. The function $g_\eta(z)$ decays as $2/3z^2$ as the magnitude of z approaches infinity. Because of the exponential, then, and the fact that r is always positive, the integral can be closed in the upper half plane. Taking proper account of the singularity structure of the integrand, Eq. (20) is replaced by

$$J_1(\kappa, \alpha, r) = \frac{1}{2ir} \lim_{\eta \to 0} \left\{ \int_{\Gamma_r} \frac{q g_\eta(q/2\kappa)}{q^2 + \alpha^2} e^{iqr}\, dq + \int_{\Gamma_-} \frac{q g_\eta(q/2\kappa)}{q^2 + \alpha^2} e^{iqr}\, dq + \int_{\Gamma_+} \frac{q g_\eta(q/2\kappa)}{q^2 + \alpha^2} e^{iqr}\, dq \right\}, \tag{21}$$

where the contours are illustrated in Fig. 2.

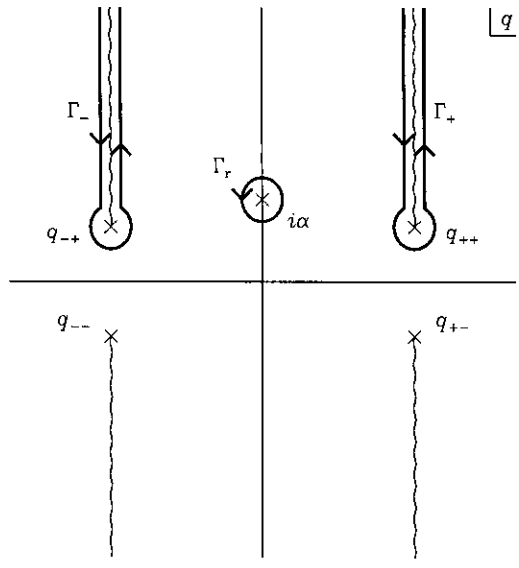

FIG. 2. Contours for the integral in Eq. (21). The quantities $q_{\pm\pm}$ are equal to $2\kappa z_{\pm\pm}$.

The integral over Γ_r is along a closed contour about the root, $q = i\alpha$ (recall that α is positive), and can be evaluated with the theorem of residues:

$$\int_{\Gamma_r} \frac{q g_\eta(q/2\kappa)}{q^2+\alpha^2} e^{iqr}\, dq = \pi i g_\eta(i\alpha/2\kappa) e^{-\alpha r} \underset{\eta\to 0}{\sim} \pi i \left[1 + \left(\frac{2\kappa}{\alpha} + \frac{\alpha}{2\kappa}\right) \arctan(\alpha/2\kappa)\right] e^{-\alpha r}. \tag{22}$$

For the integral over Γ_+, note that the integrand differs on either side of the branch cut only in the logarithmic part of $g_\eta(z)$. On the left side of the cut, $z = (1 + se^{-3\pi i/2})$, while on the right side, $z = (1 + se^{\pi i/2})$, with the variable s ranging from η to ∞. The difference in the function $g_\eta(z)$ on the two sides of the cut is therefore given by

$$g_\eta(1 + se^{\pi i/2}) - g_\eta(1 + se^{-3\pi i/2}) = -\frac{\pi i}{2}\frac{s^2 - 2is}{1 + is}. \tag{23}$$

This leads to

$$\int_{\Gamma_+} \frac{q g_\eta(q/2\kappa)}{q^2+\alpha^2} e^{iqr}\, dq = 2\kappa^2 \pi e^{2i\kappa r} \int_\eta^\infty \frac{(s^2 - 2is)e^{-2\kappa r s}}{-4\kappa^2 s^2 + 8\kappa^2 is + (4\kappa^2 + \alpha^2)} ds \underset{\eta\to 0}{\sim} -\frac{\pi e^{2i\kappa r}}{4\kappa r} - \frac{\pi}{2}\left(1 + \frac{\alpha^2}{4\kappa^2}\right) \int_{-i}^{-i+\infty} \frac{e^{-2\kappa r u}}{u^2 - \alpha^2/4\kappa^2} du. \tag{24}$$

A similar expression can be derived for the integral over Γ_- and there results

$$J_1(\kappa,\alpha,r) = \frac{\pi}{2r}\left[1 + \left(\frac{2\kappa}{\alpha} + \frac{\alpha}{2\kappa}\right)\arctan(\alpha/2\kappa)\right] e^{-\alpha r} - \frac{\pi \sin(2\kappa r)}{4\kappa r^2} + \frac{\pi}{4ir}\left(1 + \frac{\alpha^2}{4\kappa^2}\right) \left\{\int_{C_1} \frac{e^{-2\kappa r u}}{u^2 - \alpha^2/4\kappa^2} du + \int_{C_3} \frac{e^{-2\kappa r u}}{u^2 - \alpha^2/4\kappa^2} du\right\}, \tag{25}$$

where C_1 and C_3 are portions of the contour illustrated in Fig. 3. Because of the connection between the paths and the closed contour, the sum of integrals remaining in Eq. (25) can be replaced by the integral over the entire closed contour minus those over the portions C_2 and C_4 (see Fig. 3). Due to the exponential in the integrand, the integral over C_2 vanishes. A little rearrangement then gives the final result

$$J_1(\kappa,\alpha,r) = \frac{\pi}{2r}\left\{\left[1 - \frac{4\kappa^2 + \alpha^2}{2\kappa\alpha}\arctan(2\kappa/\alpha)\right] e^{-\alpha r} - \frac{\sin(2\kappa r)}{2\kappa r} + \frac{4\kappa^2 + \alpha^2}{2\kappa\alpha}\alpha r\, F_2(\alpha r, 2\kappa r)\right\}, \tag{26}$$

where

$$F_2(x,y) \equiv \int_0^y \frac{\cos w}{w^2 + x^2} dw. \tag{27}$$

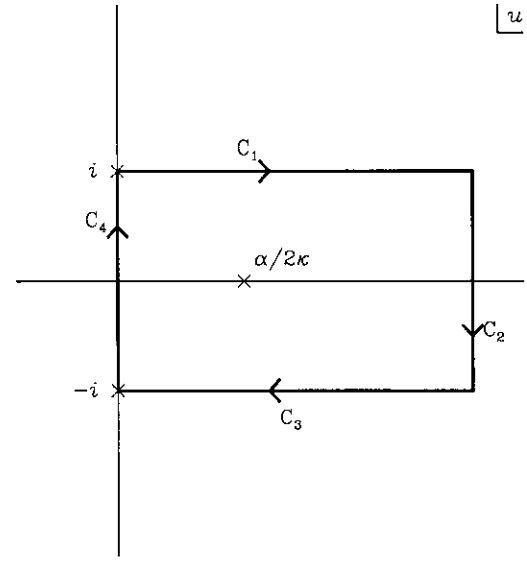

FIG. 3. Contour used for the integrations over u in Eq. (25). The portion C_2 represents a segment at infinity where the integrand vanishes strongly.

It is possible to express the function $F_2(x, y)$ in terms of exponential integrals with complex arguments (see Section 4). However, from a computational viewpoint, the integral on the right-hand side of Eq. (27) is more easily handled by numerical means. Therefore, this function is retained in this form.

3. EVALUATION OF $J_2(\kappa, \alpha, r)$

Evaluation of the second of Eqs. (10b) can be performed by simply taking a derivative. In particular,

$$\begin{aligned} J_2(\kappa, \alpha, r) &= -\frac{\partial}{\partial \alpha} J_1(\kappa, \alpha, r) \\ &= \frac{\pi}{2\alpha r}\left\{-(1-\alpha r)e^{-\alpha r} + \cos(2\kappa r)\right. \\ &\quad - \frac{(4\kappa^2 - \alpha^2) + \alpha r(4\kappa^2 + \alpha^2)}{2\kappa\alpha} \arctan(2\kappa/\alpha) e^{-\alpha r} \\ &\quad + \frac{4\kappa^2 + \alpha^2}{2\kappa\alpha} \alpha r F_1(\alpha r, 2\kappa r) \\ &\quad \left. + \frac{4\kappa^2 - \alpha^2}{2\kappa\alpha} \alpha r F_2(\alpha r, 2\kappa r)\right\}, \end{aligned} \tag{28}$$

where

$$F_1(x, y) \equiv \int_0^y \frac{w \sin w}{w^2 + x^2}\, dw. \tag{29}$$

Combining the quantities appropriately gives

$$\begin{aligned} G(\kappa, \alpha, r) &= \frac{\pi}{2r}\left\{\cos(2\kappa r) - \frac{\sin(2\kappa r)}{\kappa r} + (1+\alpha r)e^{-\alpha r}\right. \\ &\quad - \frac{(12\kappa^2 + \alpha^2) + \alpha r(4\kappa^2 + \alpha^2)}{2\kappa\alpha} \arctan(2\kappa/\alpha) e^{-\alpha r} \\ &\quad + \frac{4\kappa^2 + \alpha^2}{2\kappa\alpha} \alpha r F_1(\alpha r, 2\kappa r) \\ &\quad \left. + \frac{12\kappa^2 + \alpha^2}{2\kappa\alpha} \alpha r F_2(\alpha r, 2\kappa r)\right\}. \end{aligned} \tag{30}$$

4. NUMERICAL EVALUATION OF THE FUNCTIONS

The whole purpose of solving these integrals in closed form is to provide an efficient means of evaluating these quantities on the computer. Other than the functions $F_1(x, y)$ and $F_2(x, y)$, evaluation of $G(\kappa, \alpha, r)$ is straightforward. Since κ and α are always positive, it can be shown that the value of the arctangent is always between 0 and $\pi/2$. There will therefore be no ambiguity about an added multiple of π in the evaluation of this part. The evaluation of the remaining functions will now be considered.

Before discussing their evaluation in general, it is useful to mention some limiting cases of the functions $F_1(x, y)$ and $F_2(x, y)$. For this purpose, these functions can be expressed in terms of the better studied exponential integral functions [9]

$$\begin{aligned} F_1(x, y) &= \frac{1}{2}\{e^x \operatorname{Im}[E_1(x+iy)] \\ &\qquad + e^{-x}(\pi + \operatorname{Im}[E_1(-x+iy)])\} \\ F_2(x, y) &= \frac{1}{2x}\{-e^x \operatorname{Im}[E_1(x+iy)] \\ &\qquad + e^{-x}(\pi + \operatorname{Im}[E_1(-x+iy)])\}. \end{aligned} \tag{31}$$

The exponential integrals are defined by

$$E_1(z) = \int_z^\infty \frac{e^{-t}}{t}\, dt \quad (|\arg z| < \pi), \tag{32}$$

where the path of integration does not cross the negative real axis or contain the origin. The relations (31) assume that both x and y are real and positive. From these expressions, the following limiting forms are obtained:

$$\begin{aligned} F_1(x, y) &\underset{x\to 0}{\sim} \operatorname{Si}(y) - \frac{\pi}{2}x \\ F_2(x, y) &\underset{x\to 0}{\sim} \frac{\pi}{2x} - \left(\frac{\cos y}{y} + \operatorname{Si}(y)\right) + \frac{\pi}{4}x \end{aligned} \tag{33a}$$

$$\begin{aligned} F_1(x, y) &\underset{y\to 0}{\sim} \frac{y^3}{3x^2} \\ F_2(x, y) &\underset{y\to 0}{\sim} \frac{y}{x^2} - \frac{(2+x^2)}{6x^4} y^3 \end{aligned} \tag{33b}$$

$$\begin{aligned} F_1(x, y) &\underset{x\to \infty}{\sim} \frac{\sin y - y\cos y}{x^2} \\ F_2(x, y) &\underset{x\to \infty}{\sim} \frac{\sin y}{x^2} \end{aligned} \tag{33c}$$

$$\begin{aligned} F_1(x, y) &\underset{y\to \infty}{\sim} \frac{\pi}{2} e^{-x} - \frac{\cos y}{y} \\ F_2(x, y) &\underset{y\to \infty}{\sim} \frac{\pi}{2x} e^{-x} + \frac{\sin y}{y^2} \end{aligned} \tag{33d}$$

$$\begin{aligned} F_1(\lambda x, \lambda y) &\underset{\lambda\to 0}{\sim} (y - x \arctan(y/x))\lambda \\ F_2(\lambda x, \lambda y) &\underset{\lambda\to 0}{\sim} \frac{\arctan(y/x)}{\lambda x} \end{aligned} \tag{33e}$$

$$F_1(\lambda x, \lambda y) \underset{\lambda\to\infty}{\sim} -\frac{y\cos(\lambda y)}{\lambda(x^2+y^2)}$$
$$F_2(\lambda x, \lambda y) \underset{\lambda\to\infty}{\sim} \frac{\sin(\lambda y)}{\lambda(x^2+y^2)}. \tag{33f}$$

The sine integral in these expressions is defined by [9]

$$\mathrm{Si}(z) = \int_0^z \frac{\sin t}{t}\,dt. \tag{34}$$

These relations can be used to find the limiting forms for the function $G(\kappa, \alpha, r)$. They are

$$G(\kappa, \alpha, r) \underset{\kappa\to 0}{\sim} \frac{4\pi}{3\alpha^2 r}\{4 - (4+\alpha r)e^{-\alpha r}\}\kappa^2$$
$$G(\kappa, \alpha, r) \underset{\kappa\to\infty}{\sim} \frac{\pi}{r}(2+\alpha r)e^{-\alpha r}$$
$$G(\kappa, \alpha, r) \underset{\alpha\to 0}{\sim} \frac{\pi}{r}\left(2 + \pi\kappa r - \cos(2\kappa r) - \frac{\sin(2\kappa r)}{2\kappa r} - 2\kappa r\,\mathrm{Si}(2\kappa r)\right)$$
$$G(\kappa, \alpha, r) \underset{\alpha\to\infty}{\sim} \frac{\pi}{\alpha^2 r^3}\left(-4\cos(2\kappa r) + \frac{\sin(2\kappa r)}{\kappa r}\right)$$
$$G(\kappa, \alpha, r) \underset{r\to 0}{\sim} 2\pi\kappa \arctan(2\kappa/\alpha)$$
$$G(\kappa, \alpha, r) \underset{r\to\infty}{\sim} \frac{\pi(12\kappa^2+\alpha^2)\sin(2\kappa r)}{4\kappa r(4\kappa^2+\alpha^2)}. \tag{35}$$

When the values of the arguments are close to any of these limiting cases, evaluation of $G(\kappa, \alpha, r)$ on the computer is best handled with the explicit formulas given above. Otherwise, numerical integration of the functions $F_1(x, y)$ and $F_2(x, y)$ can be done effectively. Specifically, define the integer quantity $n_s = \mathrm{int}(y/2\pi)$. Then

$$F_1(x,y) = \int_0^{2\pi} \sin w \sum_{n=1}^{n_s} \frac{2(n-1)\pi + w}{[2(n-1)\pi + w]^2 + x^2}\,dw + \int_{2\pi n_s}^{y} \frac{w\sin w}{w^2+x^2}\,dw$$
$$F_2(x,y) = \int_0^{2\pi} \cos w \sum_{n=1}^{n_s} \frac{1}{[2(n-1)\pi + w]^2 + x^2}\,dw + \int_{2\pi n_s}^{y} \frac{\cos w}{w^2+x^2}\,dw. \tag{36}$$

Breaking up the integral into two parts ensures that the oscillatory part of the integrand is appropriately sampled. The numerical integrals are performed accurately using Romberg integration [10].

Code has been written to evaluate these quantities and tested for their accuracy and speed. An important concern in the speed of the calculations is clearly the Romberg integration used in the evaluation of $F_1(x, y)$ and $F_2(x, y)$. If too many grid points are needed for this part of the calculation, a lot of time could be used. By varying the number of grid points, it was found that 33 points are sufficient for six-digit accuracy except where x is small (less than 0.01). In this case, however, the limiting form given in Eq. (32a) gives satisfactory results. Calculations on a DEC 3000/400 required 4×10^{-4} s per evaluation of $G(\kappa, \alpha, r)$.

5. CONCLUSIONS

The objective of this work is to derive an efficient means of computing the atom-centered integrals defined in Eq. (6). To perform OTF calculations on a solid state system, a self-consistent field algorithm is used. In this algorithm, it is necessary to compute these integrals for each grid point of the unit cell at each iteration. Hence, the efficiency of this computation is an important concern.

Code has been written to perform these calculations. Using a modest grid size for the numerical integration, six-digit accuracy is achieved with little computation time.

At present, code is being developed for the application of the OTF method to solid state systems. An initial application is the palladium metal crystal. Because of the fundamental difference between the OTF and Hartree–Fock approximations, problems peculiar to the OTF approximation have arisen and are being investigated. Reports of progress in this effort will be presented at a later stage.

REFERENCES

1. L. R. Pratt, G. G. Hoffman, and R. A. Harris, *J. Chem. Phys.* **88,** 1818 (1988).
2. G. G. Hoffman and L. R. Pratt, *Proc. R. Soc. London A* ***435,*** 245 (1991).
3. G. G. Hoffman, unpublished work; G. G. Hoffman and L. R. Pratt, Comparison of electron density functional models, *Mol. Phys.* **82,** 245 (1994).
4. L. H. Thomas, *Proc. Cambridge Philos. Soc. A* **68,** 542 (1927).
5. E. Fermi, *Z. Phys.* **48,** 73 (1928).
6. This field is based on the work of H. Hohenberg and W. Kohn, *Phys. Rev.* **136,** B864 (1964).
7. A good overview is given in W. Yang and R. G. Parr, *Density Functional Theory of Atoms and Molecules* (Oxford Press, New York, 1989).
8. See A. L. Fetter and J. D. Walecka, *Quantum Theory of Many-Particle Systems* (McGraw–Hill, New York, 1971), p. 175.
9. N. Nielsen, *Die Gammafunktion, Band II, Theorie des Integrallogarithmus und Verwandter Transzendenten* (Chelsea, New York, 1965).
10. W. H. Press, B. P. Flannery, S. A. Teukolsky, and W. T. Vetterling, *Numerical Recipes* (Cambridge Univ. Press, Cambridge, UK, 1986), p. 114.